Design of Micromixers Using CFD Modelling

J. Aubin[a*], D.F. Fletcher[b] and C. Xuereb[a]

[a]Laboratoire de Génie Chimique UMR 5503 CNRS, 5 rue Paulin Talabot BP-1301,
Toulouse Cedex 1 31106, France
[b]Department of Chemical Engineering, The University of Sydney,
Sydney, N.S.W. 2006, Australia

Aubin J., Fletcher D.F. and Xuereb C., Design of Micromixers Using CFD Modelling, *Chem. Eng. Sci.*, **60**, 2503-2516 (2005)

Abstract

The effect of various geometrical parameters of a grooved staggered herringbone micromixer on the mixing performance has been investigated using Computational Fluid Dynamics. Mixing quality has been quantified with spatial data statistics, maximum striation thickness and residence time analyses. The results show that the number of grooves per mixing cycle does not affect the mixing quality in an important way. On the other hand, a larger groove depth and width allow the maximum striation thickness to be rapidly reduced, without increasing the pressure drop across the mixer. Wide grooves, however, create significant dead zones in the microchannel, whereas deep grooves improve the spatial mixing quality.

Keywords: Mixing, micromixer, laminar flow, Computational Fluid Dynamics (CFD), striation thickness, spatial analysis.

1. Introduction

Micromixers play a significant role in micro chemical processing and are employed in a multitude of tasks, including blending, emulsification and suspension, as well as for chemical reaction and also in combination with integrated heat exchangers. Due to the small dimensions of the micro channels, the flow is predominantly laminar and mixing is therefore limited by molecular diffusion. In order to effectively mix in a reasonable time, fluids must be manipulated so that the interfacial surface area between the fluids is increased massively and the diffusional path is decreased, enhancing the molecular diffusion to complete the mixing process (Ehrfeld *et al*., 2000). A number of mechanisms exist for fluid contacting and mixing, including multilamination, splitting and recombination, hydrodynamic focussing, T- and Y-junctions (Ehrfeld *et al*., 2000), as well as chaotic advection (Beebe *et al*., 2001; Lui *et al*., 2000; Stroock *et al*., 2002).

Due to the relatively young age of microreactor engineering, common design rules for micromixers have not yet been developed. However, one can see that apart from their minute size, microreactors are merely continuous laminar flow reactors, which suggests that design approaches for mixing in micro channels could be

* Corresponding author: Tel: +33 (0)5 34 61 52 43, Fax: +33 (0)5 34 61 52 53, Email: Joelle.Aubin@ensiacet.fr

dealt with in a similar manner to that of laminar mixing in macro scale pipe flow. In undisturbed laminar flow; the streamlines run parallel to one another and there is no convective mixing in the radial or tangential directions, which results in a high degree of *spatial* inhomogeniety. In addition, the parabolic velocity profile of the laminar flow gives rise to *temporal* inhomogeneities, which translates into wide residence time distributions. Thus in order to disturb the flow and facilitate mixing in laminar pipeline flow, in-line devices or static mixers are inserted into the channel. The best designs of such devices create a high degree of plug flow, thus decreasing temporal inhomogeneities, whilst achieving homogenisation in the radial direction, which increases the spatial homogeneity (Etchells and Meyer, 2004). The design of micromixers, which are comparatively similar devices at a much smaller scale, can be looked at in the same manner, whereby the aim is to provide sufficient spatial and temporal mixing as fast as possible.

A number of methods are commonly used in order to characterize both the spatial and temporal mixing performance of large-scale static mixing devices, for example: the coefficient of variation and the intensity of segregation (Hobbs and Muzzio, 1997, 1998a, 1998b; Mickaily-Huber *et al*., 1996; Rauline *et al*., 2000; Zalc *et al*., 2002), Poincaré sections (Hobbs and Muzzio, 1998a, 1998b), striation thickness (Fourcade *et al*., 2001) and residence time distributions (Hobbs and Muzzio, 1997; Nauman *et al*., 2002; Visser *et al*., 1999). These can be implemented experimentally and/or numerically – the numerical approaches have been detailed in Aubin *et al*. (2003).

Over the past few years, a number of studies using different types of micromixers have been carried out with the aim of characterising the mixer performance using various experimental techniques, such as fluorescent microscopy and special chemical reactions, as well as CFD simulations to trace particle trajectories (Beebe *et al*., 2001; Bertsch *et al*., 2001; Ehrfeld *et al*., 1999; Lui *et al*., 2000; Stroock *et al*., 2002a, 2002b). As we discussed in a previous paper (Aubin *et al*., 2003), these methods are indirect and enable mainly qualitative comparisons of micromixers but they do not give quantitative data, such as mixing times or mixing lengths. Furthermore, they rarely make use of the characterization methods that have been developed for macro-scale static mixers. In Aubin *et al*. (2003), we have used a numerical approach for quantifying the mixing quality in micromixers, which is based on a spatial analysis method that has previously been used for assessing the performance of macro-scale static mixers. This statistical approach employs quadrat analysis of Lagrangian particle trajectories whereby two-dimensional planes in the mixer are divided into equal sized quadrats and the number of particles within each quadrat is recorded. At each plane, the variance of particle distribution with respect to an ideally homogenised distribution is calculated. This in turn gives an idea of the channel length necessary to obtain a particular degree of mixing. Although the methodology described above is useful for quantifying the rate at which particles are spread throughout the mixer, it is highly dependent on the size and number of quadrats used, as well as the number of particles traced (Lui *et al*., 1994). If the quadrats are too large, the technique will quantify mixing only on a coarse scale and thus small scale flow patterns that are smaller than the quadrat size will be filtered out. On the other hand, if the quadrats are very small, a very large number of particles would be required, which would demand an extremely long computational time. In Aubin *et al*. (2003), the micromixer geometries investigated gave strikingly different flow patterns and therefore the quadrat size and particle number that were employed were sufficient for the comparison of the two mixers. In the current study, the differences between the various micromixer flow patterns are much smaller and a higher degree of resolution is thus required for better quantification.

In our previous paper, we characterised the mixing quality in a diagonally grooved micromixer (DM) and a staggered herringbone micromixer (SHM) using Computational Fluid Dynamics (CFD). It was shown that the SHM mixes much more efficiently and in a shorter time than the DM. In the current study, we have decided to study numerically the effect of different geometrical parameters of the SHM on the mixing quality, with the aim of improving the mixer design. We present an alternative method for quantifying the level of spatial homogenisation in micromixers, which is based on a statistical method called nearest-neighbour analysis. A measure of the reduction in maximum striation thickness as a function of mixer length is also used to quantify distributive mixing. Temporal mixing is then assessed by the determination of residence time distributions. Lastly, the effect of the various geometrical modifications on the pressure drop is examined.

Sections 2-4 describe the various micromixer geometries investigated, as well as the numerical and characterization methods employed in this work. A detailed analysis of the results is then presented in section 5 and the conclusions are given in section 6.

2. Mixer Geometry

The mixer geometries used in this study are based on that proposed by Strook *et al*. (2002) and have an off-centered herring bone pattern in the channel floor (Figure 1), which creates a transverse velocity component in the flow field. The mixer is composed of several mixing cycles, whereby a mixing cycle comprises two sequential regions of grooves, i.e. two half-cycles. The direction of asymmetry of the herringbones switches with respect to the centreline of the channel every half cycle. The mixer consists of a rectangular channel (w = 200 μm, h = 77 μm, L = 0.01 m) with grooves of depth, d_g, and width, W_g, which have a wave vector of $2\pi/100$ μm^{-1}. In this work, the groove depth, the groove width and the number of grooves per cycle, N_g, were varied in order to understand their effect on the mixing quality. Table 1 presents the different cases investigated and the values of the geometrical parameters.

Table 1: Geometrical parameters of the different micromixers investigated.

Case	Groove Depth, d_g	Groove Width, W_g (μm)	Number of Grooves per Cycle
Reference (Stroock *et al*., 2002)	0.23h	50	20
1 (d_g = 0.30h)	**0.30h**	50	20
2 (d_g = 0.35h)	**0.35h**	50	20
3 (W_g = 25 μm)	0.23h	**25**	20
4 (W_g = 75 μm)	0.23h	**75**	20
5 (N_g = 10)	0.23h	50	**10**
6 (N_g = 30)	0.23h	50	**30**

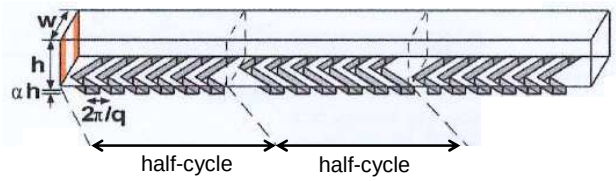

Figure 1: Geometry of the staggered herringbone micromixer (Stroock *et al*., 2002).

3. Numerical Methods

The numerical simulation of the flow and mixing in the micromixers has been performed using ANSYS-CFX5 (ANSYS, 2003). This is a general purpose commercial CFD package that solves the Navier-Stokes equations using a finite volume method via a coupled solver. The analysis procedure has been carried out in two steps. Firstly, the velocity and pressure fields in the mixer are solved. These values are then used to calculate particle trajectories within the flow field.

3.1 Flow Computation

A mesh composed of approximately 1 330 000 hexahedral elements (1 500 000 nodes) was used. A preliminary grid convergence study was carried out in order to verify that the solution is grid independent. The boundary condition at the channel inlet was a uniform velocity profile with $v_x = 0.02$ ms^{-1} and $v_y = v_z = 0$ ms^{-1}. This corresponds to a laminar flow regime with a Reynolds number (Re) ≅ 2. At the outlet, a constant pressure condition (P = 0) was imposed and no-slip boundary conditions were applied at all walls. Water at 25 °C and 1 atm was used as the operating fluid. The CFX5.6 solver was used to solve the steady-state momentum and continuity equations for the fluid flow in the micromixers. The advection terms in each equation were discretized using a bounded second order differencing scheme to minimise the effects of numerical diffusion. Simulations were typically considered converged when the normalised residuals for the velocities fell below 1×10^{-6}.

3.2 Particle Tracking

In this study, a 50-50% mixture of mass-less fluid particles in the flow is followed using a Lagrangian particle tracking method in order to quantify the mixing quality. Initially, 2480 evenly distributed particles are place on the right-hand side of the mixer inlet. This approach avoids the introduction of numerical diffusion which results if a scalar is tracked, which confuses the mixing behaviour. The movement of the particle tracers in the flow is determined by integration the vector equation of motion for each particle:

$$\frac{\mathrm{d}\mathbf{x}}{\mathrm{d}\,t} = v(\mathbf{x}) \tag{1}$$

In order to obtain a sufficient degree of accuracy when integrating the equation of motion, a fourth order Runge-Kutta scheme with adaptive step size has been employed. Furthermore, a restitution coefficient of unity is applied to the microchannel walls. This avoids particle trajectories being trapped near the walls where the local velocity is close to zero (less than 2 % of particles are stopped between the inlet and the outlet of the mixer).

4. Characterization Methods

4.1 Spatial Mixing

Spatial mixing has been characterized by two methods. The first is a variation of nearest-neighbour analysis, which is used in spatial data statistics and measures the distance between a particular coordinate and a tracer particle. The second method measures the reduction in the maximum striation thickness at different positions along the microchannel.

4.1.1 Analysis using Point-Event Distances

Nearest-neighbour analysis, like quadrant analysis, is used in spatial data statistics to study the spatial distribution of point patterns on a plane (Diggle, 1983). The nearest-neighbour method differs from quadrant analysis in that it is based on the distance between each point and its nearest neighbour and that it does not require the studied region to be divided into quadrants. Several different nearest-neighbour methods exist; some are based on the mean distance between the two nearest particle locations compared with a randomly distributed set of particle locations, others use the distance between a randomly chosen point and the nearest particle position (point-event distance). Such analysis methods have been widely used in ecology (e.g., the study of the distribution of trees) and biology (e.g., the study of the distribution of cell nuclei). Concerning other scientific disciplines however, it appears that spatial data analysis has been employed only occasionally in materials science to study the distribution of microporosity in alloy materials (e.g., Anson and Gruzleski, 1999).

In this study, we have carried out a statistical analysis using an adapted point-event distance methodology. Instead of choosing random point coordinates and calculating their distance to the nearest particle tracer positions, we have used a set of uniformly spaced points that represent a perfectly homogeneous mixture. In a two-dimensional plane, the most uniform pattern for a set of points occurs in a regular hexagonal tessellation with a point at the centre of each hexagon, Figures 2 and 3.

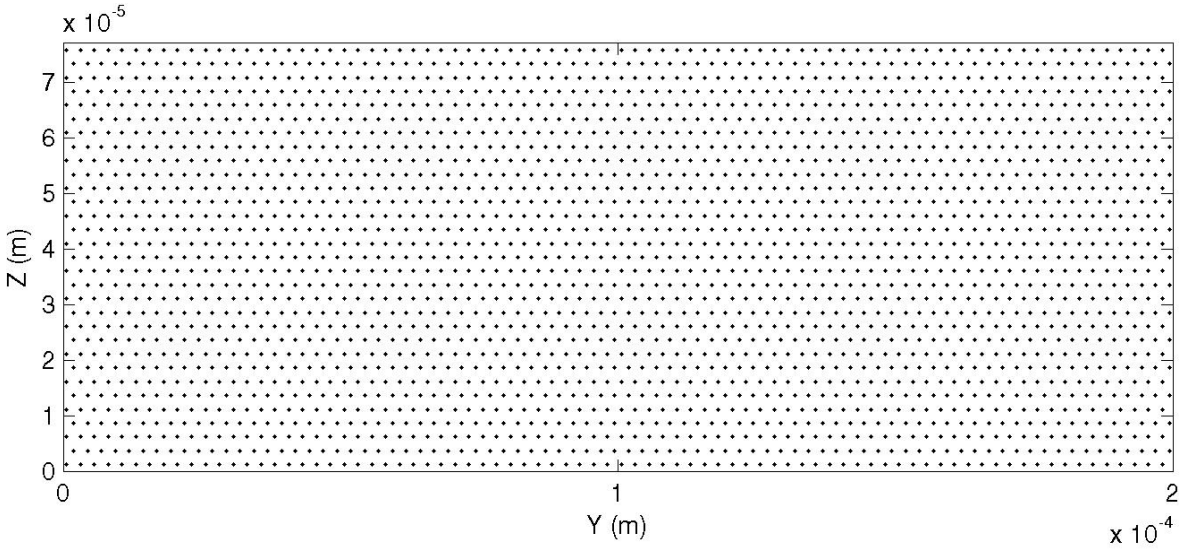

Figure 2: Uniform pattern for a set of points occurring in a regular hexagonal tessellation.

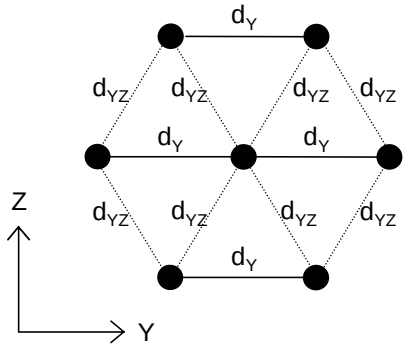

Figure 3: Hexagonal tessellation for the calculation of the mean inter-point distance.

In this work, we have used 2480 tracer particles to analyse the flow. To obtain the most uniform distribution of this number of points, we arrange them as an 80×31 array in the Y-Z plane. Considering the Y-Z dimensions of the micro channel, this gives an inter-point distance of $d_y = 2.50$ µm in the Y-direction and $d_{yz} = 2.78$ µm in the direction of the Y-Z vector. An approximation of the mean inter-point distance of this uniform array of points can be calculated as the mean distance between all points in a regular hexagonal tessellation with a point at the centre (Equation 2 & Figure 3).

$$\bar{d}_R = \left(4d_Y + 8d_{YZ}\right)/12 \tag{2}$$

For different cross-sectional planes along the micro mixer channel, point-particle location distances, d_i, are determined by calculating the distance between each particular location of the evenly distributed points, P_i (y_i, z_i), and the location of the nearest particle tracer, P_t (y_t, z_t):

$$d_i = \sqrt{\left(y_i - y_t\right)^2 + \left(z_i - z_t\right)^2} \tag{3}$$

From this the spread of the point-particle location distances from the expected mean distance of the uniform point pattern can be determined using:

$$\text{var} = \frac{1}{N-1}\sum_{i=1}^{N}\left(d_i - \bar{d}_R\right)^2 \tag{4}$$

A 'well mixed' criterion has been set such that for any point-particle location distance, d_i, which is less than the expected mean distance, $\bar{d}_R$, a value equal to $\bar{d}_R$ is assigned to d_i. This means that variance value of 0 corresponds to a uniform spatial distribution of tracer particles.

4.1.2 Striation Thickness

The maximum striation thickness at different positions along the micromixer has been measured at the mid-height of the channel. To do this, it has been assumed that all particles which have a Z-coordinate between 35 µm and 40 µm are at the mid height of the channel. The distance in the Y-direction, Δy, between two consecutive particles is then calculated. The distance Δy is then tested by fixing a threshold value, Δy_T, in order to determine whether two consecutive particles are part of the same striation or not. In this study, the value of Δy_T has been set to 5 µm, which is the same resolution as in the Z-direction. The following test is then executed:

$\Delta y \le \Delta y_T$: Consecutive particles belong to the same striation, f $(x) = 1$
$\Delta y > \Delta y_T$: Consecutive particles belong to different striations, f $(x) = 0$ (5)

Figure 4(a) shows the function f (x) for the reference case at the position X = 0.04 cm along the micromixer as an example. It can be seen that this method for determining the thickness of striations correctly depicts the corresponding particle tracer pattern that is observed in Figure 4(b). The data from the function f (x) are then used to calculate the maximum striation thickness at any position along the micromixer.

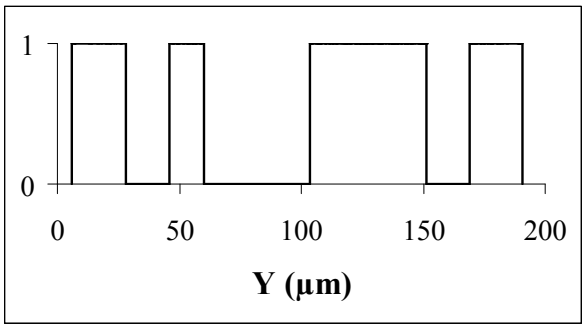

(a)

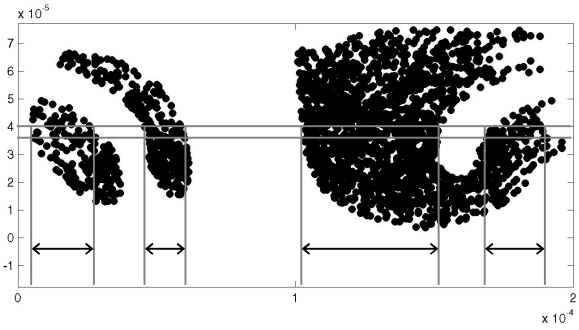

(b)

Figure 4: Determination of the maximum striation thickness for the reference case at X = 0.4 cm: (a) function f(x); (b) corresponding particle tracer pattern with observed striation thicknesses.

4.2 Temporal Mixing

4.2.1 Residence Time Distribution (RTD)

The RTD for the fluid flowing through the various micromixer geometries was calculated by determining the particle trajectories as described in paragraph 3.2, and by recording the particle residence times after 1 cm of micromixer length. This allows the calculation of a residence time distribution, E(t), as described by Folger (1992):

$$E(t) = \frac{\Delta N}{N} \cdot \frac{1}{\Delta t} \tag{6}$$

where ΔN is the number of particles that have a residence time in the mixer between time t and t+Δt and N is the total number of particles released at the entry of the microchannel. The cumulative residence time distribution, F(T) can then be calculated as:

$$F(T) = \sum_{t \le T} E(t).\Delta t \tag{7}$$

The residence times of the particles were then normalised by the expected mean residence time, $\tau = V/Q$, in the mixer to obtain the normalised residence time Θ. The residence time distribution and the cumulative distribution as a function of Θ are then expressed as:

$$E(\Theta) = \tau . E(t) \tag{8}$$

$$F(\Theta) = \sum_{\theta \le \Theta} E(\theta).\Delta\theta \tag{9}$$

5. Results and Discussion

5.1 Visualisation of Mixing

In order to visualise the mixing phenomena in the various micromixer geometries, the particle locations at different axial positions along each mixer are plotted, as shown in Figures 5-7. A detailed description of the mechanism of mixing in this type of micromixer has already been given in Aubin *et al*. (2003) and will therefore not be repeated here.

Figure 5 compares the effect of groove depth on the mixing patterns in the micro channel. Several observations are noted as the groove depth increases (from Figure 5(a) to Figure 5(c)). In the first part of the microchannel, the flux of particles from the right-hand side to the left-hand side increases, this in turn favours the exchange of particles between the left-hand and right-hand sides of the channel. Consequently, the rate of decrease of the maximum striation thickness increases as the groove depth increases and spatial homogenisation of the particle tracers occurs more quickly.

The groove width has an important effect on the spatial mixing quality as can be seen in Figure 6. If the grooves are very narrow (Figure 6(b)), the exchange of fluid between the left-hand and right-hand sides of the channel is very poor because the amount of fluid that enters the grooves and attains a transverse velocity component is reduced. The resulting mixing pattern is very orderly, with a finger-like structure being created at the end of each mixing cycle. When the grooves are wide compared with the reference case, as shown in Figure 6(c), the mixing pattern is very irregular. The exchange of fluid between both sides of the mixer is important and the rate of reduction of the largest striation increases considerably. However, it is also noted that for the case of wide grooves, the distribution of particles is much less uniform than in the reference case. The particles tend to gravitate towards the centre of the channel, leaving the upper and lower corners void of particles. This suggests the possible presence of dead zones, which lack circulation. Such a hypothesis can be verified using the RTD analysis.

Figure 7 shows the effect of the number of grooves per cycle on the mixing quality. When the number of grooves per cycle is halved with respect to the reference case, short fine finger-like striations are formed at the end of each cycle. The fineness of these striations would clearly facilitate molecular diffusion. Nevertheless, the largest striation at the centreline of the channel is not that much different from that of the reference case geometry. When the number of grooves per cycle is greater than that of the reference case, the finger-like structures are relatively thick. However, they have time to be folded upon themselves, which then decreases the striation thickness. Nevertheless, after 1 cm of mixer length, the maximum striation thickness appears to be more or less similar to that present in the reference geometry.

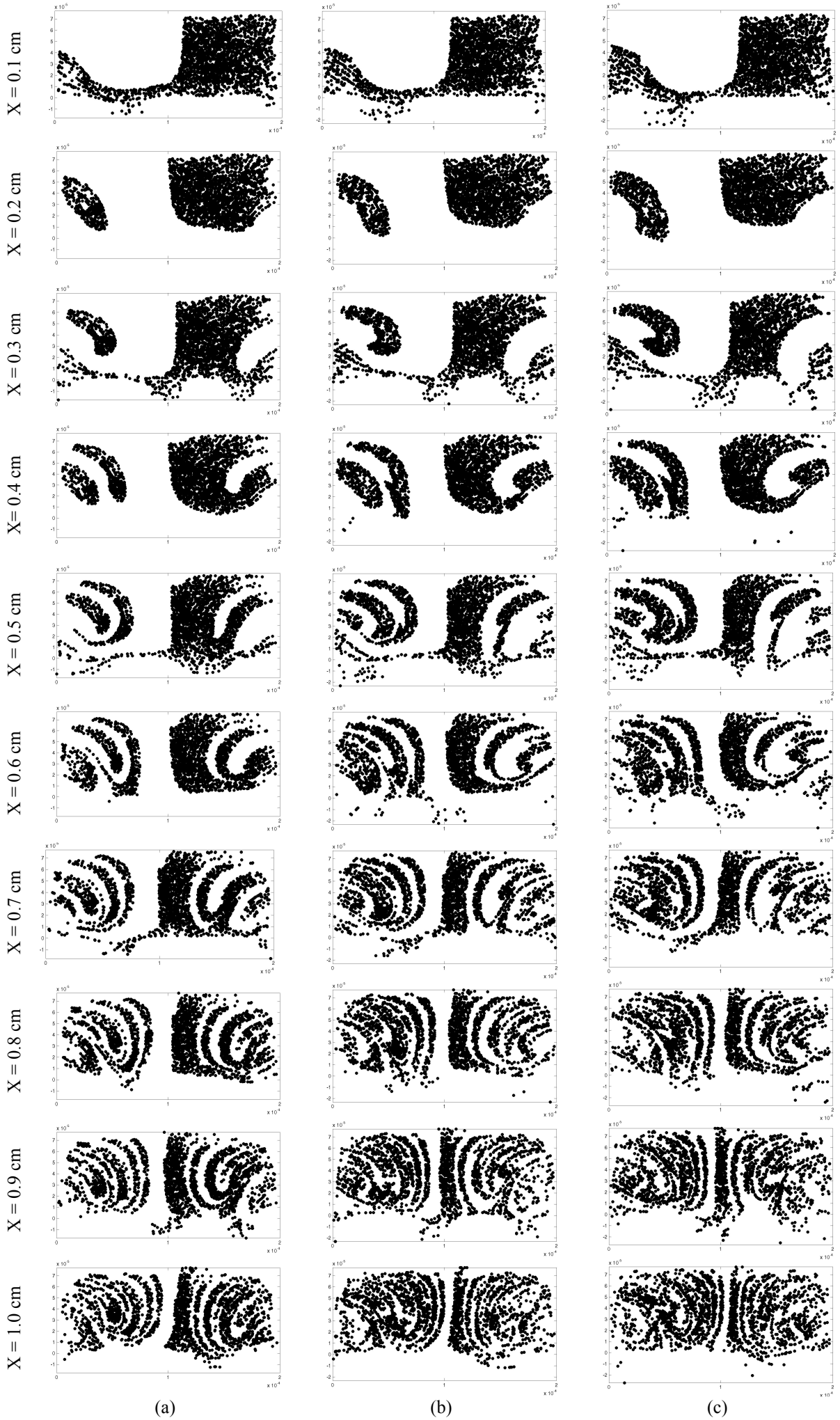

Figure 5: Effect of the groove depth, d_g, on mixing patterns: (a) reference case ($d_g = 0.23h$); (b) $d_g = 0.30h$; (c) $d_g = 0.35h$.

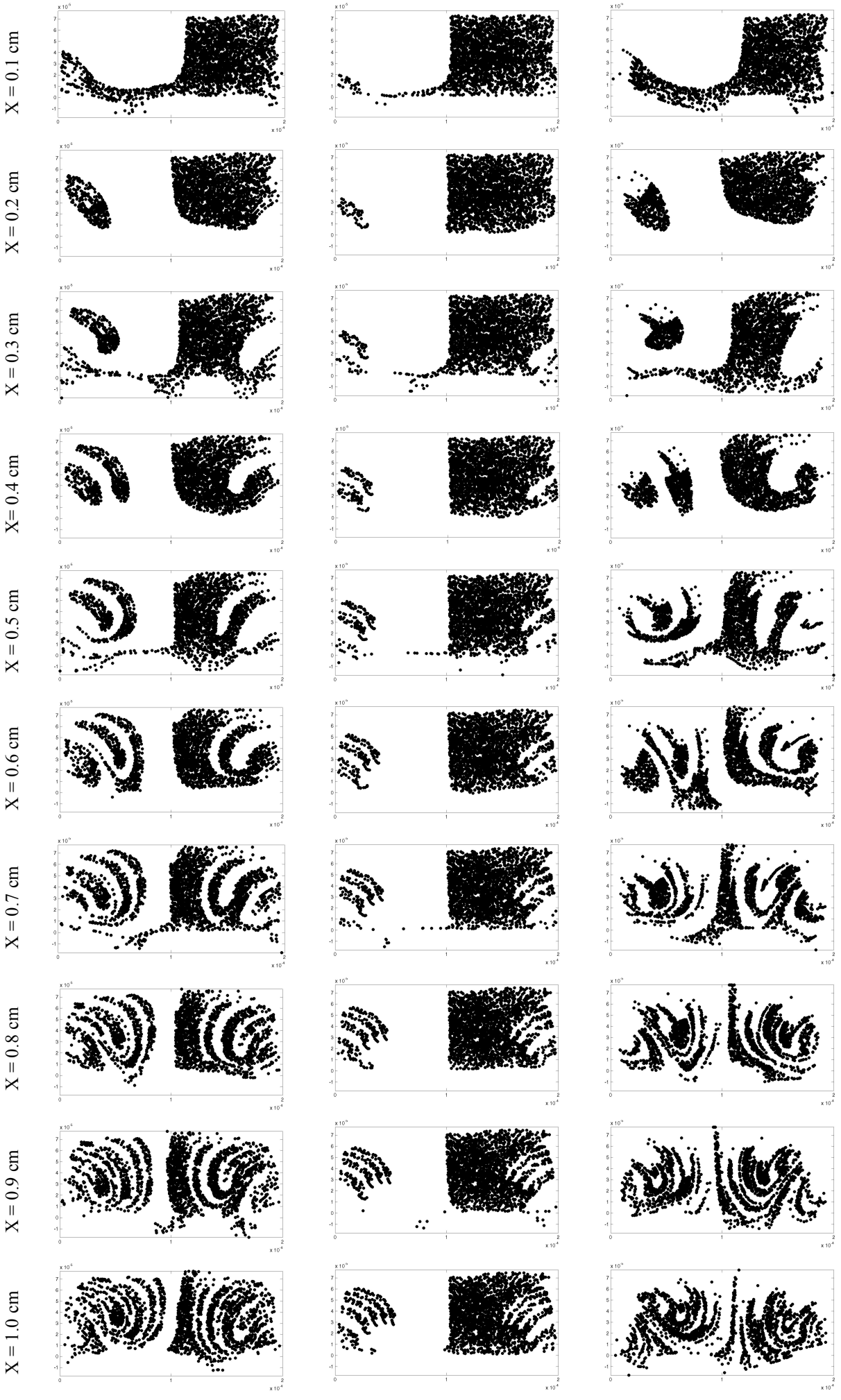

Figure 6: Effect of the groove width, W_g, on mixing patterns: (a) reference case (W_g = 50 μm); (b) W_g = 25 μm; (c) W_g = 75 μm.

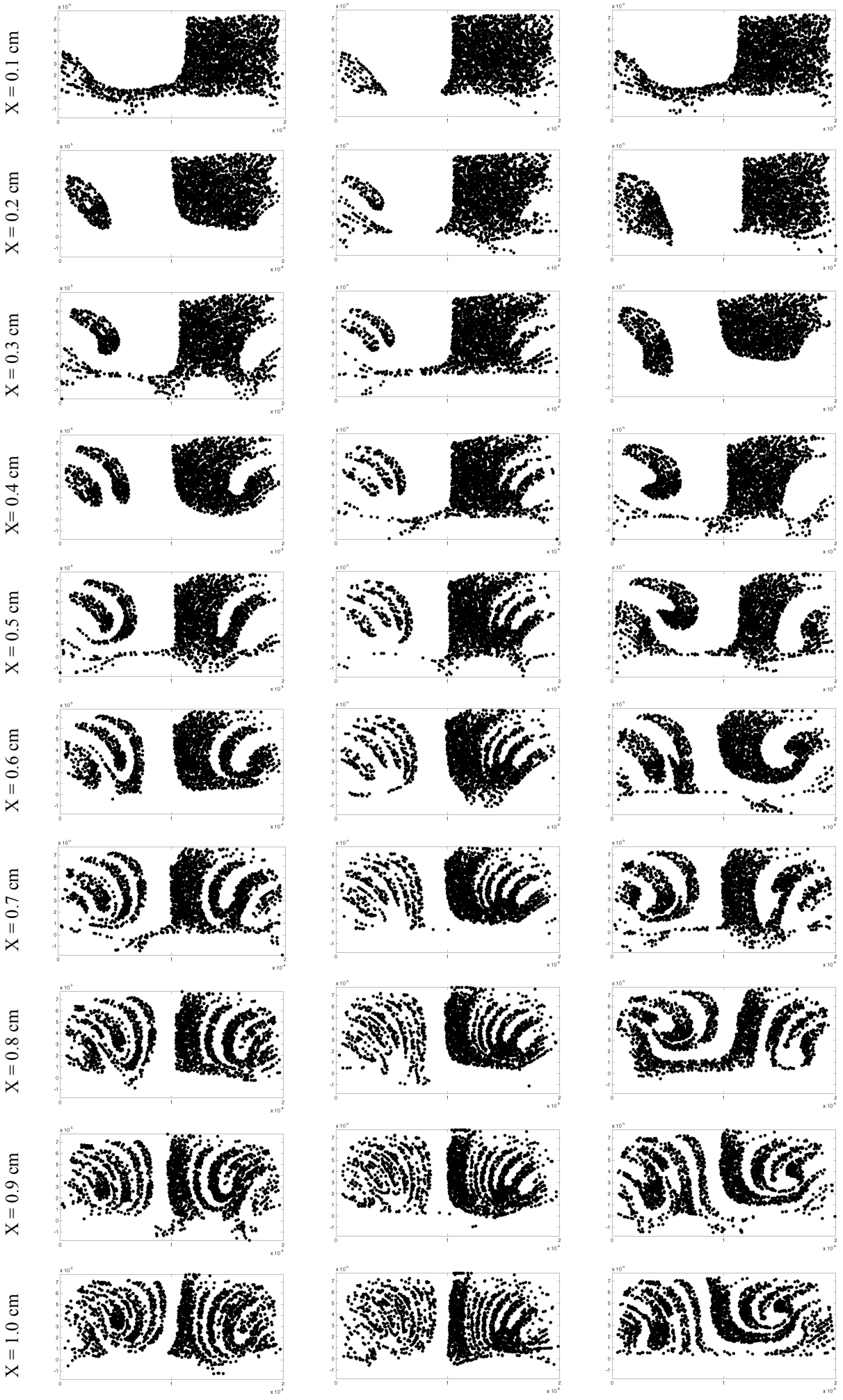

Figure 7: Effect of the number of grooves, N_g, per cycle on mixing patterns: (a) reference case ($N_g = 20$); (b) $N_g = 10$; (c) $N_g = 30$.

5.2 Quantification of Spatial Mixing

In order to evaluate the homogeneity of the mixing patterns presented in section 5.1, the spread of the particle patterns from the ideal uniformly distributed pattern was quantified by calculating the variance as described in section 4.1.1. At each position along the micromixer, the variance, var, is normalised by the variance at the entry of the channel, var_o. A normalised variance value of 0 corresponds to a uniform spatial distribution of tracer particles and thus good mixing, whilst a value of 1 indicates that no spatial mixing has occurred compared with the initial state of the system.

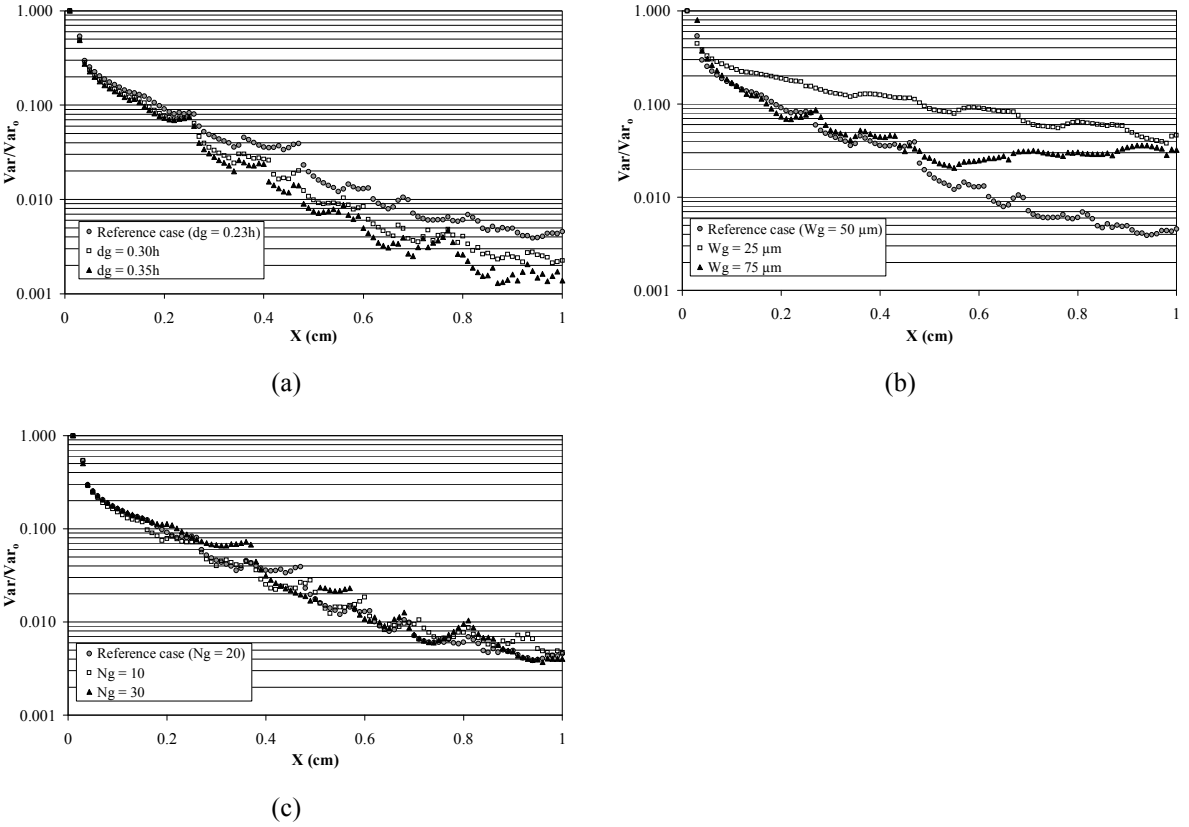

Figure 8: Effect of geometrical parameters on the normalised variance: (a) effect of groove depth; (b) effect of groove width; (c) effect of number of grooves per cycle.

Figure 8 shows the effect of the different geometrical parameters on the normalised variance at different positions along the micromixer. In Figure 8(a), it can be seen that the spatial mixing quality improves as the groove depth increases. At approximately position X = 0.85 cm, the variation in the normalised variance appears to plateau off for the three cases and thus the spatial pattern of the tracer varies very little. This suggests that from this position onwards, the striation patterns are being modified much more slowly by advection and that the final phase of mixing will be limited by molecular diffusion. It can be seen in Figure 8(b) that quantitatively the groove width has a strong effect on the homogenisation. When the grooves are very narrow, spatial mixing is very slow and at least 2 cm of mixer length would be needed to obtain the same quality of mixing achieved in only 1 cm of the reference case mixer geometry. The curve corresponding to the wide grooved micromixer is quite unique. The mixing quality appears to evolve in a similar manner to the reference case mixer until approximately X = 0.45. After this point, the tracer tends to accumulate near the centre of the channel creating

empty zones in the channel corners, thus causing the normalised variance to plateau off. The number of grooves per cycle does not appear to have a very important effect on the spatial distribution of the tracer, as shown in Figure 8(c). It is however noticeable that towards the end of the mixer, the curves for cases $N_g = 10$ and $N_g = 30$ are still varying considerably compared with the reference case. This suggests that advection is still playing an important role in the modification of the flow structures.

5.3 Striation Thickness

The reduction in maximum striation thickness as a function of the micromixer length for the various geometries is shown in the semi-log plots given in Figure 9. The dotted line indicates a striation thickness of 10 μm, which has been fixed as a reference. The time for a striation to mix by pure molecular diffusion can be estimated by:

$$t_{diff} = \frac{s^2}{D} \tag{10}$$

where s is the striation thickness and D is the molecular diffusion. For a striation of width 10 μm and a typical molecular diffusion in liquids of 2×10^{-9} m^2/s, the mixing time by diffusion is approximately 0.05 s. With the flow rate studied here, this is less than one tenth of the mean residence time in the mixer and in this time, the fluid will be convected only about 0.1 cm. It can thus be assumed that a sufficient level of mixing is obtained in the mixers when the maximum striation thickness is 10 μm or less.

Figure 9(a) compares the effect of different groove depths on the maximum striation thickness. As observed in the particle patterns in Figure 5, the rate of reduction of the maximum striation thickness is proportional, but not linearly, to the groove depth. The results suggest that a maximum groove depth exists whereby the decrease in the maximum striation thickness is no longer significantly improved. Quantitatively, a striation thickness of 10 μm is obtained after approximately 0.84 cm of mixer when $d_g = 0.35h$ and 0.92 cm when $d_g = 0.30h$. This means that one can expect very good mixing in both geometries with just 1 cm of mixer length. In order to attain a striation thickness of 10 μm in the reference case mixer, however, a much longer micromixer is required, around 1.2 cm and one would expect complete mixing within 1.3 cm of mixer length. The graphs in Figure 9(b), which compare the effect of groove width on the striation thickness, are remarkably different, as suggested by the particle patterns in Figure 6. Firstly, it can be seen that the maximum striation thicknesses for the three cases do not decrease in an exponential manner, as is expected for typical chaotic flow (Ottino, 1989). This is most apparent for the geometry with wide grooves. Here, the rate of reduction of the maximum striation thickness greatly increases along the length of the micromixer. In this geometry, a striation thickness of 10 μm is obtained after approximately 0.75 cm of mixer, which is much less than the length required by the reference case geometry. For the case with narrow grooves, a relatively long mixer is needed to attain the same quality of mixing. The effect of the number of grooves per cycle on the striation thickness is compared in Figure 9(c). The results quantitatively show the striation thickness does not depend on this geometrical parameter, which confirms the qualitative observations made in Figure 7.

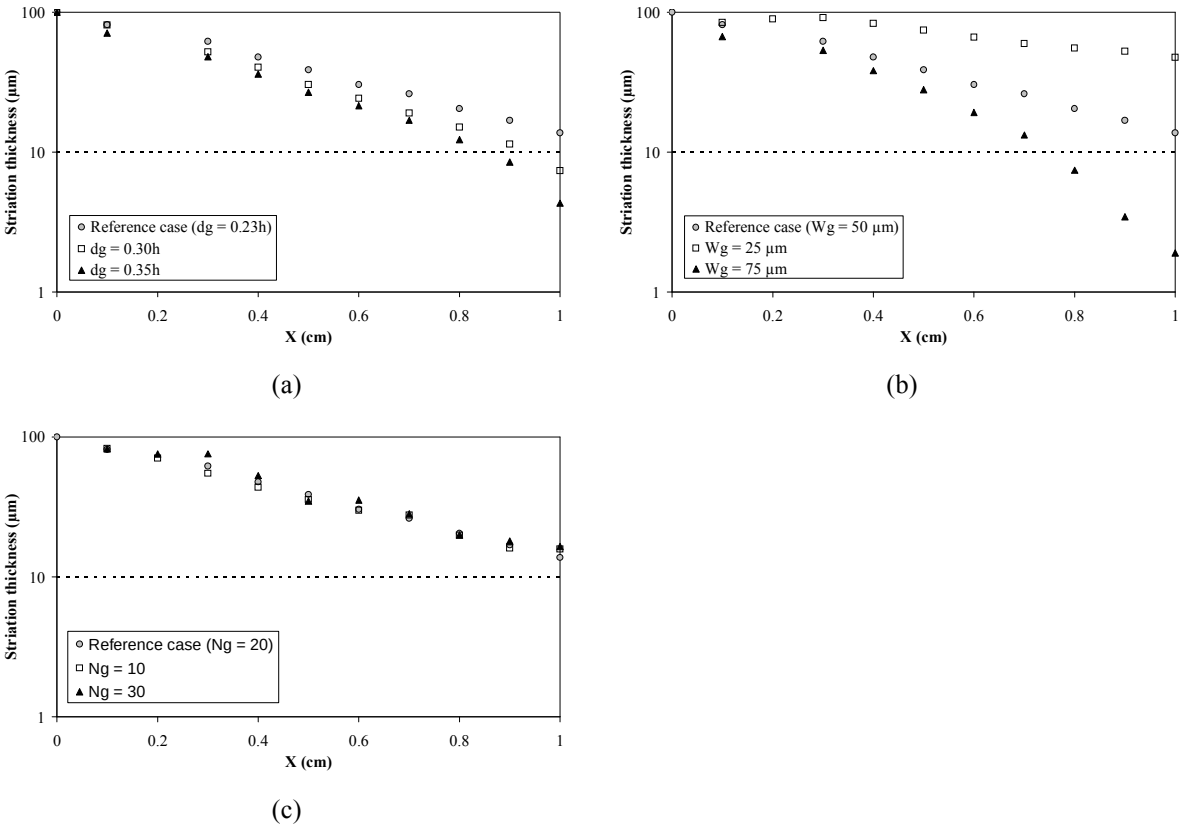

Figure 9: Evolution of the maximum striation thickness: (a) effect of groove depth; (b) effect of groove width; (c) effect of number of grooves per cycle.

5.4 Residence Time Distributions

The cumulative residence time distributions are presented in Figure 10. It can be seen from Figures 10(a) and 10(c) that neither the groove depth nor the number of grooves per cycle affect the residence time distributions significantly. Nevertheless, it is noticed that the RTDs in these mixer geometries do deviate from the typical Poiseuille flow distribution and tend towards a plug flow distribution, which means that the grooves present in channels act as flow inverters and equalize the residence times as macro-scale static mixers do. The curves in Figure 10(b) are however quite different from one another. When the grooves are narrow, they have little effect on the flow and the RTD is very close to that of Poiseuille flow. For wide grooves, however, the RTD is much closer to that of typical plug flow. As seen in the particle pattern plots in Figure 6, the tracer in the wide groove geometry moves to the centre of the microchannel, leaving zones void of particles in the upper and lower corners. This means that particles move with much similar velocities as they are avoiding the low velocities close to the channel walls, thus the tracer RTD tends towards a plug flow RTD. In order to verify the existence of possible dead zones in this micromixer geometry, the mean residence time of the tracer has been compared with the expected mean residence time ($\tau = V/Q$), as shown in Table 2. The mean residence time in significantly lower (15 %) than the expected mean residence time, whereas for the other mixer geometries there is generally not more the 5 % difference. This means that for the wide groove geometry, the effective volume of the micromixer is decreased, which confirms the presence of dead zones in the channel corners. It should be stressed that the mass-less tracer used here does not take into account any mixing via molecular diffusion. For

the simulation of a scalar concentration or the experimental mixing of a dye, however, one would expect the tracer to mix into these dead zones via molecular diffusion but very slowly compared with the rest of the channel.

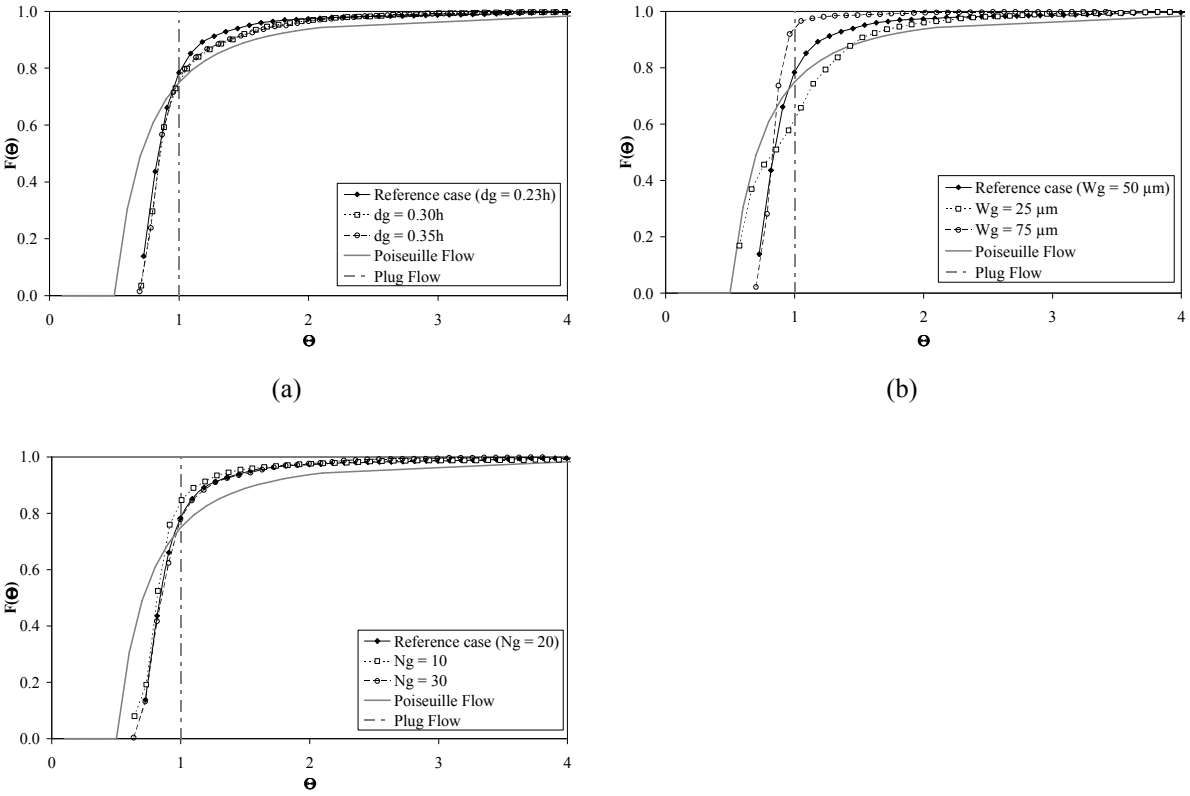

Figure 10: Effect of geometrical parameters on the cumulative residence time distributions: (a) effect of groove depth; (b) effect of groove width; (c) effect of number of grooves per cycle.

Table 2: Mean residence time, t_m, compared with the expected mean residence time, τ, for the various micromixer geometries.

Case	Expected Mean Residence Time, τ, (s)	Mean Residence Time, t_m, (s)
Reference (Stroock *et al.*, 2002)	0.551	0.521
1 (d_g = 0.30h)	0.565	0.561
2 (d_g = 0.35h)	0.575	0.568
3 (W_g = 25 µm)	0.524	0.509
4 (W_g = 75 µm)	0.571	0.486
5 (N_g = 10)	0.547	0.500
6 (N_g = 30)	0.522	0.517

5.5 Pressure Drop

The pressure drop, ΔP, across the various micromixers is presented in Table 3. It is observed that the groove depth and the number of grooves per cycle have almost no effect on the pressure drop across the micromixer: deviations from the pressure drop across the reference case geometry are less than 1 %. The width of the grooves, however, has a small effect on the pressure drop: an increase in groove width decreases ΔP.

Table 3: Pressure drop across the various micromixer geometries.

Case	Pressure Drop, ΔP (Pa)
Reference (Stroock *et al.*, 2002)	428.5
1 (d_g = 0.30h)	426.8
2 (d_g = 0.35h)	425.8
3 (W_g = 25 µm)	454.8
4 (W_g = 75 µm)	393.2
5 (N_g = 10)	433.3
6 (N_g = 30)	430.5

6. Conclusions

CFD simulations have been performed in order to investigate the effect of various geometrical parameters in a staggered herringbone micromixer and to hence indicate how the design of such micromixers can be modified to improve the mixing quality. Qualitative and quantitative analyses of the spatial mixing quality show that the groove depth and the groove width have the greatest influence on homogenisation. On the other hand, the number of grooves per cycle does not affect the mixing quality. As the groove depth increases, homogenisation increases. If the groove width is very narrow, the flow in the microchannel is hardly affected by the transversal velocity component and spatial mixing is very poor. For wide grooves however, homogenisation does not necessarily improve since the tracer tends to accumulate near the centre of the mixer leaving dead zones in the corners of the channel. A measure of the reduction of maximum striation thickness has also allowed the quantification of spatial mixing. It was found that for grooves deeper than 30 % of the channel height, mixing is greatly improved. For the operating conditions studied here, complete mixing can occur within 1 cm of the microchannel. The wide groove mixer was also found to very efficient in decreasing the striation thickness. On the other hand, the number of grooves per cycle does not modify the reduction in striation thickness. The temporal mixing quality was investigated using cumulative residence time distributions. The results show that the grooves present on the microchannel floor allow flow inversion and equalisation of residence times, compared with typical Poiseuille flow. It is also confirmed that the wide grooves give rise to important dead zones in the microchannel volume. Lastly, a comparison of the pressure drop across the micromixers shows that the groove depth and the number of grooves per cycle do not affect this parameter.

Thus, in order to improve the mixing quality in staggered herringbone micromixers, one is advised to use a mixer with deep grooves, having a depth of 30-40 % of the channel height. This promotes both spatial

homogenisation and the reduction of striation thickness, without increasing the pressure drop across the mixer. A groove width of 50 μm (wider grooves increase dead zones in the mixer) and 20 grooves per cycle appear to be adequate, as proposed originally by Strook *et al*. (2002).

Future work will be directed toward the experimental investigation of micromixers using visualisation techniques and micro-Particle Image Velocimetry, with the aim of providing detailed validation data.

7. References

Anson, J.P., Gruzleski, J.E., (1999). The Quantitative Discrimination between Shrinkage and Gas Microporosity in Cast Aluminium Alloys Using Spatial Data Analysis, *Mater. Charact*., 43, 319-335.

ANSYS, (2003). www.ansys.com/cfx

Aubin, J., Fletcher, D.F., Bertrand, J., Xuereb C., (2003). Characterization of the Mixing Quality in Micromixers, Chem. Eng. Technol., 26, 12, 1262-1270.

Beebe, D.J., Adrian, R.J., Olsen, M.G., Stremler, M.A., Aref, H., Jo, B.-H., (2001). Passive Mixing in Microchannels: Fabrication and Flow Experiments, *Mec. Ind.*, 2, 343-348.

Bertsch, A., Heimgartner, S., Couseau, P., Renaud, P., (2001). Static Micromixers Based on Large-Scale Industrial Mixer Geometry, *Lab on a Chip*, 1, 56-60.

Diggle, P.J., (1983). Statistical Analysis of Spatial Point Patterns, Academic Press, London.

Ehrfeld, W., Golbig, K., Hessel, V., Löwe, H., Richter, T., (1999). Characterization of Mixing in Micromixers by a Test Reaction: Single Mixing Units and Mixer Arrays, *Ind. Eng. Chem. Res*., 38, 1075-1082.

Ehrfeld, W., Hessel, V., Löwe, H., (2000). Microreactors: New Technology for Modern Chemistry, Wiley-VCH, Weinheim.

Etchells, A.W., Meyer, C.F., (2004). Mixing in Pipelines, in: Paul, E.L., Atiemo-Obeng, V.A. and Kresta, S.M. (Eds.), Handbook of Industrial Mixing: Science and Practice, John Wiley & Sons Inc., Hoboken NJ, p. 391.

Folger, H.S., (1992). Elements of Chemical Reaction Engineering, 2nd Ed., PTR Prentice Hall, Englewood Cliffs NJ.

Fourcade, E., Wadley, R., Hoefsloot, H.C.J., Green, A., Iedema, P.D., (2001). CFD Calculation of Laminar Striation Thinning in Static Mixer Reactors, *Chem. Eng. Sci*., 56, 6729-6741.

Hobbs, D.M., Muzzio, F.J., (1997). The Kenics Static Mixer: A Three-Dimensional Chaotic Flow, *Chem. Eng. J*., 67, 153-166.

Hobbs, D.M., Muzzio, F.J., (1998a). Optimization of a Static Mixer Using Dynamical Systems Techniques, *Chem. Eng. Sci*., 53, 18, 3199-3213.

Hobbs, D.M., Muzzio, F.J., (1998b). Reynolds Number Effects on Laminar Mixing in the Kenics Static Mixer, *Chem. Eng. J*., 70, 93-104.

Li, H.Z., Fasol, C., Choplin, L., (1996). Hydrodynamics and Heat Transfer of Rheologically Complex Fluids in a Sulzer SMX Static Mixer, *Chem. Eng. Sci*., 51, 10, 1947-1955.

Lui, M., Muzzio, F.J., Peskin, R.L., (1994). Quantification of Mixing in Aperiodic Chaotic Flows, *Chaos, Solitons & Fractals*, 4, 6, 869-893.

Lui, R.H., Stremler, M.A., Sharp, K.V., Olsen, M.G., Santiago, J.G., Adrian, R.J., Aref, H., Beebe, D.J., (2000). Passive Mixing in a Three-Dimensional Serpentine Microchannel, *J. Micro. Elec. Mech. Sys.*, 9, 2, 190-197.

Mickaily-Huber, E.S., Bertrand, F., Tanguy, P., Meyer, T., Renken, A., Rys, F.S., Wehrli, M., (1996). Numerical Simulations of Mixing in an SMRX Static Mixer, *Chem. Eng. J.*, 63, 117-126.

Nauman, E.B., Kothari, D., Nigam, K.D.P., (2002), Static Mixers to Promote Axial Mixing, *Trans IChemE Chem. Eng. Res. Des*., 80A, 1-5.

Ottino, J.M., (1989). The Kinematics of Mixing: Stretching, Chaos and Transport, Cambridge University Press, Cambridge.

Rauline, D., Le Blévec, J-M., Bousquet, J., Tanguy, P.A., (2000). A Comparative Assessment of the Performance of the Kenics and SMX Static Mixers, *Trans IChemE Chem. Eng. Res. Des*., 78A, 389-396.

Stroock, A.D., Dertinger, S.K.W., Ajdari, A., Mezic, I., Stone, H.A., Whitesides, G.M., (2002a). Chaotic Mixer for Microchannels, *Science*, 295, 647-651.

Stroock, A.D., Dertinger, S.K., Whitesides, G.M., Ajdari A., (2002b). Patterning Flows Using Grooved Surfaces, *Anal. Chem*., 74, 20, 5306-5312.

Visser, J.E., Rozendal P.F., Hoogstraten, H.W., Beenackers, A.A.C.M., (1999). Three-Dimensional Numerical Simulation of Flow and Heat Transfer in the Sulzer SMX Static Mixer, *Chem. Eng. Sci*., 54, 2491-2500.

Zalc, J.M., Szalai, E.S., Muzzio, F.J., Jaffer, S., (2002). Characterization of Flow and Mixing in an SMX Static Mixer, *AIChE J*., 48, 3, 427-436.